Modelling Using Neural Networks and Dynamic Position Control for Unmanned Underwater Vehicles

◉ Melek Ertogan[1], ◉ Philip A. Wilson[2]

[1]İstanbul Technical University Faculty of Maritime, Department of Maritime Transportation and Management, İstanbul, Türkiye
[2]The University of Southampton, Ship Dynamics within Engineering and Physical Sciences, Southampton, United Kingdom

Abstract

Underwater construction, maintenance, and mapping use autonomous underwater vehicles (AUVs) for path planning, path following, and target tracking operations. However, dynamic position management and localization of AUVs are critical issues. Correct localization and dynamic position management to prevent drifts can be used to acquire information on energy efficiency, another crucial topic. In this paper, AUV dynamic modeling using experimental data and position control is studied. The experiments were implemented on a Delphin2 scaled AUV model belonging to the Engineering and Environment Faculty, University of Southampton, UK. Hover and flight style motions according to the different speeds of Delphin2 were implemented in the test tank. Nonlinear coupled mathematical models were studied using shallow neural networks. The models are formed into depth-pitch and heading motion black-box models using the shallow neural network (SNN) algorithm. Proportional integral derivative control of heading motions and depth-pitch motion simulation studies were applied to the SNN model.

Keywords: Autonomous underwater vehicle, Shallow neural networks, Black box modelling, Dynamic position control

1. Introduction

Autonomous underwater vehicles' (AUVs) research and application topics include localization, path following, target tracking, underwater mapping, and dynamic position management. Energy efficiency is a key issue that can be resolved by combining precise localization with dynamic position control to halt drifts.

The goal of this study is to create and test an algorithm for dynamic position controllers for AUVs. The scaled Delphin2 AUV model from the Engineering and Environment Faculty at the University of Southampton in the UK was used for the experiments [1-6]. To provide dynamic position control during hover and flight-style operations underwater, the local position definition of AUVs is a crucial challenge.

Delphin2 has an inertial measurement unit (IMU), a depth pressure sensor, a sounding altimeter, a mechanical scanning sonar, and a global positioning system (GPS). GPS does not work underwater or in closed areas such as tank tests. The IMU includes a 3D accelerometer, gyroscope, and magnetometer. The heading-pitch-depth motions of Delphin2 can be measured in tank tests and underwater applications.

Surge and sway motions of an AUV cannot be measured during underwater operations for this research study because an ultra-short baseline (USBL) positioning system cannot be used for tank tests because of the wall effect.

An over-actuated design enables the Delphin2 AUV model to perform various missions, from hover-style operation at zero or slow speeds to flight-style operation at forward speeds up to approximately 1 m/s.

Hover and flight style motions according to the different speeds of Delphin2 were implemented in the tank. Nonlinear coupled mathematical models were studied using experimental data. Proportional integral derivative (PID) control of heading and depth-pitch motions simulation studies were performed on the nonlinear mathematical model. Previous control studies on Delphin2, such as model predictive control (MPC) depth-pitch motion control [3]

To cite this article: M. Ertogan, and P. A. Wilson. "Modelling Using Neural Networks and Dynamic Position Control for Unmanned Underwater Vehicles." *Journal of ETA Maritime Science*, vol. 12(1), pp. 64-73, 2024.

and sliding mode control heading motion control [6], were implemented.

The feedback signals were collected in the tank tests from the sensors, a sounding altimeter, a pressure depth sensor, and an IMU, according to set values on the actuator, including the vertical and horizontal tunnel thrusters, the vertical and horizontal control surfaces as the tails, and the propeller. The input-output test data were used to form nonlinear coupled mathematical models. The models were formed in two groups: altitude-pitch and heading motion black-box models using a shallow neural network (SNN) algorithm [7]. This nonlinear coupled mathematical model was used to develop a dynamic position control design. The five actuator control signals must be calculated online by a controller system using 3D depth-pitch-heading motions for the over-actuated Delphin2.

2. Literature Review

Sensor data fusion for navigation AUVs has received much attention in the literature because their localization remains a challenge. Underwater navigation techniques most commonly employed include long baseline (LBL) with IMU, USBL, and Doppler velocity log (DVL) sensors.

Because of wall effects, USBL-based echo-sounding communication cannot be used in a tank or on a shallow coast. Therefore, rangefinder sensors, such as a laser-based vision feedback sensor, and sonar systems were used to calculate AUV's localization in a tank in the literature. With the aid of an IMU and a laser-based vision system, online localization of AUVs via Kalman filtering was established [8,9]. These tests were performed in a tank. However, the laser-based vision feedback measurement range was only approximately 30 cm, and the computer vision feedback was seldom performed. After the localization study, online identification and visual control were studied [10]. Another laser-based rangefinder study was applied in a tank, and the range was approximately 5 m [11].

The position of the AUV in artificially structured environments, such as tanks, harbors, marinas, and maritime platforms, was determined using a mechanical scanning sonar with an IMU [12]. The experimental results of the simultaneous localization and mapping measurement method are presented in this thesis. To address motion-induced distortion caused by high measurement error or lengthy scan periods, a different localization of AUV based on mechanically scanned imaging sonar was investigated [13].

For open-water applications, acoustic-based USBL and LBL communication systems are used to determine the location of AUVs. According to Plueddemann et al. [14], a comparative discussion of USBL- and LBL-based AUV navigation systems is presented, along with recommendations for the limitations of USBL regarding ice area docking and shallow coast applications. The drift in the location estimation that results from DVL-based navigation makes long-range AUV navigation over 300 m considerably more challenging. To navigate underwater, a DVL is rarely used alone; instead, it is integrated with other sound sensors [15]. According to Chen et al. [16] and Paull et al. [17], survey research was conducted to investigate the mapping, navigation, and localization of AUVs.

The accuracy of AUV localization during tank tests, for example, to verify control algorithms, is compromised by wall effects when using the USBL/LBL measurement system. Additionally, the AUV's localization range, when using eye feedback, is extremely small, as is its frequency. AUV motion drifts could be caused by dead reckoning techniques. The combination of DVL and IMU for underwater vehicles was investigated using multisensor Kalman filtering [18].

There are fewer dynamic position control studies than navigation studies on AUVs. However, there have been few experimental studies on dynamic position control. Dynamic positioning systems of remotely operated vehicles and AUVs are explained comparatively [19]. Simulation studies on dynamic position control algorithms have been conducted [20,21]. In addition, experimental data were designed and verified for the 4-DOF and 6-DOF advanced controllers of AUVs [22]. The system identification (SI) method was used with experimental data for the surge and yaw modeling of AUVs [23]. Using the USBL measurement system, we demonstrated a novel optimization-based method with simulation results for dynamically placing a fully actuated AUV [24]. The neural network model reference adaptive control serves as the dynamic loop in the proposed dynamic position approach, whereas the nonlinear MPC serves as the kinematic loop.

3. Materials and Methods

3.1. AUV Characteristics

The Delphin series for AUVs was initiated in 2007 as a collaboration between the University of Southampton and the National Oceanography Centre [1]. Delphin2 was developed as a scaled model of Autosub6000 [25]. With control surfaces and a propeller, its body is designed like a torpedo. Because of the inefficiency of these types of rear control surfaces, a typical design flaw is that the AUV is unable to maintain sufficient control at zero or slow speeds. Thus, the design is expanded to include two horizontal and two vertical thrusters. Delphin2 serves as a research platform for control system development and for studying the performance of over-actuated AUVs.

A Delphin2 AUV with actuators is shown in Figure 1. This AUV has been successfully demonstrated during hover-style motions [3,4].
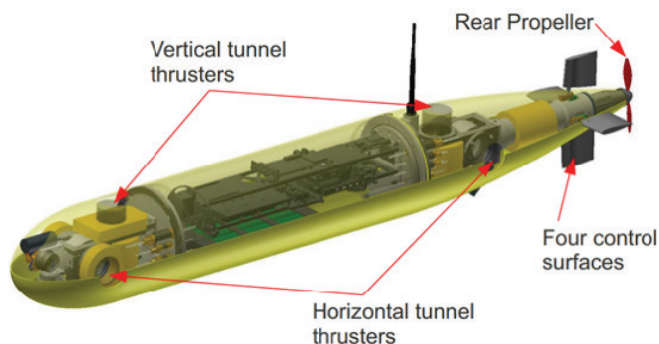

Figure 1. *Delphin2 AUV [3]*

AUV: Autonomous Underwater Vehicles

AUV Delphin2 has a mid-body diameter of 0.26 m and a length of 1.96 m, giving it a torpedo-like shape. The over-actuated Delphin2 has 7 actuators to be fully controlled. These are the propeller, the vertical and horizontal tails acting as control surfaces, the front and back vertical thrusters, and the front and rear horizontal thrusters. 3D depth-pitch-heading motion coupled control using five actuators was the focus of the research study. Consequently, it may effectively perform a range of tasks, such as survey flights at a surge speed of approximately 0-1 m/s and zero-speed hovering. In the event of a system failure, an AUV can autonomously return to the water's surface because of its small positive buoyancy. Delphin2 is typically ballasted to be buoyant at 6 N. A surge-sway motion measurement system is not present on the AUV [2].

The Delphin2 AUV has a pressure transducer rated from 0 to 5 bar to measure its depth below the free surface. For surface operation, the GPS offers a current position at a sample rate of one hertz (Hz). There is no underwater positioning option for the Delphin2 AUV. The direction and turning rate are provided at a sample rate of 20 Hz via the Xsens 4th generation MTi-30 IMU. The dynamics model is used to estimate the forward and sway velocities used in the control systems at 20 Hz to comply with the IMU. Using acoustic backscatter techniques, the altimeter and scanning-sonar track the distance between the AUV and the seabed. Delphin2 is equipped with two analog color charge-coupled device cameras, one facing ahead and the other below [2,6].

During the testing, propeller demands of uprop = {0, 10, 16, 22} were employed. These values, which roughly translate to 2.4, 4.5, and 6.15 rev/s, agree with prop. The motor control board needs these set points to operate the motor. For fully submerged operation, they roughly correspond to forward speeds of u = {0, 0.26, 0.6, 1.0} m/s or u = {0, 0.42, 0.82, 1.03} m/s for operating on the water surface. However, these speeds were calculated according to the operation time and measured distance regardless of the drifts of the Delphin2 AUV.

Accordingly, they are referred to as zero, low, mid, and high-speed cases. The thrusters function well at low and zero speeds. However, the tails work effectively at high speeds. In addition, both thrusters and tails cannot work fully effectively at mid-speeds. The effectiveness of the actuators at mid-speeds is determined with weighting functions, and the illustration is shown in Figure 2. ω_{th}, a tunnel thruster weight, and ω_s, a control surface tail weight.
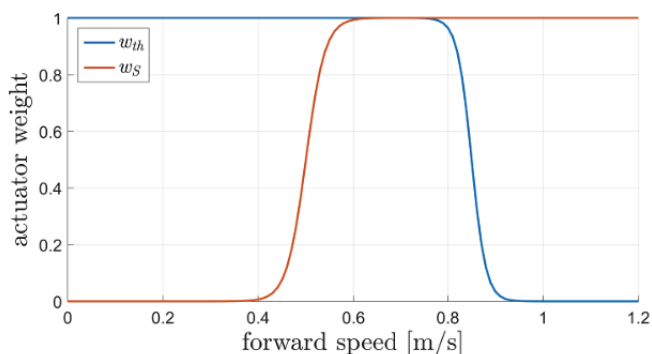

Figure 2. *Actuator weighting functions [6]*

3.2. Nonlinear Dynamic Modeling

Before control applications on the Delphin2 AUV model, dynamic modeling of the model was investigated; hence, a modeling strategywas chosen: a) nonlinear modeling is somewhat complex but might better capture actual dynamics. The coefficients can be determined using data from scaled-model testing or full-scale sea trials when the model's structure is readily accessible for the specific type of sample AUV. b) Linearized models such as state-space models or transfer functions may be adequate for the initial control design. The simplicity of these linear models is one of their advantages. However, the simulation results and actual system reactions could vary significantly.

AUV dynamics can be modeled using three different approaches: white box modeling, which employs the Navier-Stokes equations to characterize fluid structure interactions; gray box modeling, which combines experimental data with partial theoretical structures; and black box modeling, which uses only experimental data. White box modeling promises accurate predictions of AUV motions, but due to its time-consuming nature, it is not useful for control design. The term "System Identification-SI" approach refers to studies including gray and black box modeling in transdisciplinary disciplines. The SI method has proven to be very accurate

when compared with both empirical and theoretical methodologies [26]. There are few studies on AUV motion modeling using the SI technique for controller design.

The feedback signals were collected with the sensors of Delphin2, while the actuators were sending various signals in the tank experiments. These input-output data were used for nonlinear modeling of the AUV. Nonlinear coupled mathematical modeling based on the black-box model method was studied. Nonlinear depth-pitch motions and heading motions were modeled using SNNs to develop a nonlinear coupled control algorithm.

SNNs typically have fewer hidden layers, whereas deep neural networks can have dozens or even hundreds of layers. There are several layers in the network structure, including an input layer, hidden layers, and an output layer. While the hidden layer routes inputs to the output layer, the input layer handles intermediate calculations. When input values are applied, the primary goal of the network is to generate the desired output. For neural network training, the well-liked supervised learning method back propagation (BP) is propesed [27]. Due to the typical BP algorithm's slower convergence and longer training times, BP with adaptive learning rate and momentum term (BPALM) is advocated [28]. Because of the shorter training time, the BPALM, which is based on the standard BP, adjusts its learning rate and momentum rate at each iteration. Traingdx in Matlab is used to implement the BPALM method [29]. An output layer of linear neurons follows one or more hidden layers of sigmoid neurons in feedforward networks. Many layers of neurons with nonlinear transfer functions within the network enable the learning of both nonlinear and linear interactions between input and output vectors. The linear output layer indicates that the network may produce values outside the 1 to +1 range. The feedforward network models were trained using the BPALM technique [7].

In Figure 1, the actuators used as input data for modeling heading dynamics SNNs and depth-pitch dynamics SNNs are displayed. Figures 3 and 4, respectively, show the input-output data for heading dynamics and depth-pitch dynamics.
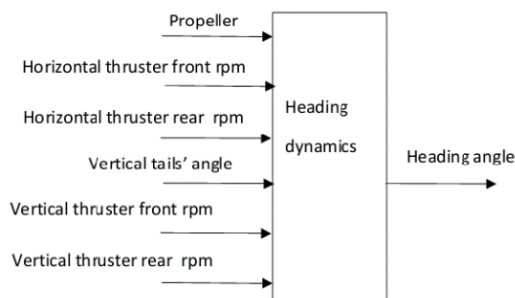

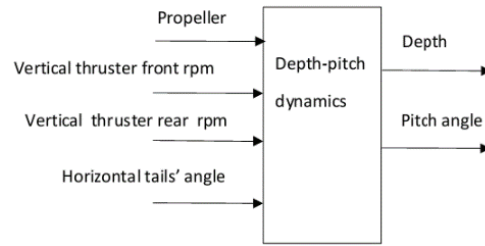**Figure 3.** *Input-output data for heading dynamics*

Figure 4. *Input-output data for depth-pitch dynamics*

Two datasets-training and test data-are prepared and used in SNN modeling. Test data are used to gage the model's performance after it has been developed using training data. Several acronyms of input and output data are employed in the following figures. The AUV's propulsion data are displayed as "uprop". During the testing, propeller demands of uprop = {0, 10, 16, 22} were employed. These values, which roughly translate to 2.4, 4.5, and 6.15 rev/s, agree with prop. The horizontal control surfaces as tail are abbreviated as "tailH", their unit is degree. The vertical control surfaces as tail are indicated as "tailV". The altimeter measures the vertical distance of the AUV from the tank bottom, and this distance is called the "altitude". In addition, the vertical thrusters located at the rear and front are abbreviated as "thrVrear" and "thrVfront", respectively. The horizontal thrusters located at the rear and front are shown as "thrHrear" and "thrHfront", respectively. All thrusters' units are rpm.

The experimental data used in the SNN modeling includes the depth, pitch, and heading motions of the AUV in hover- and flight-style conditions at various speeds. In addition, data on the actuators of the AUV, such as the horizontal-vertical thrusters and control surfaces (tails), were obtained. Depth-pitch motion and heading motion were modeled as decoupled. The depth-pitch and heading motion training data of the AUV given in Figures 5-11 are data of the same mission motions. In addition, the depth-pitch and heading motion validation/test data of the AUV given in Figures 6-12 are data of the same mission motions.
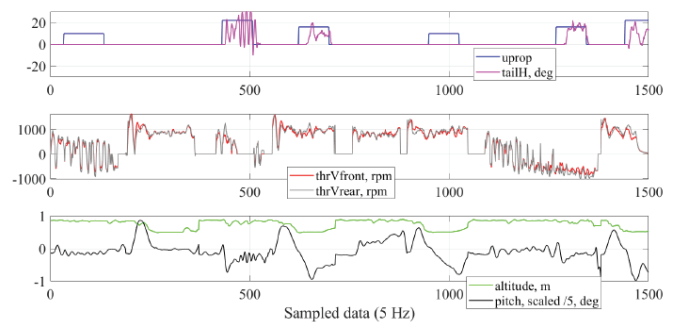

Figure 5. *SNN model training data for depth-pitch motion*
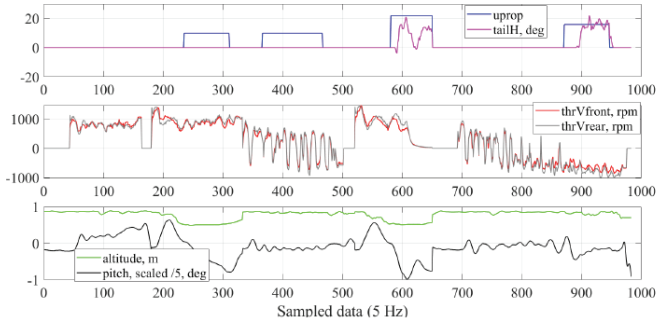
SNN: Shallow neural network

Figure 6. *SNN model test data for depth-pitch motion*

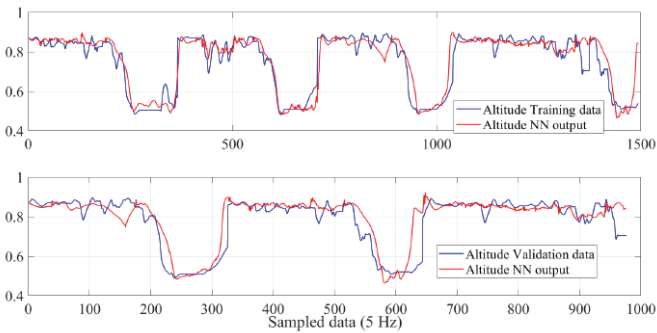*SNN: Shallow neural network*

Figure 7. *Comparison between SNN output and experimental altitude data for training and validation*
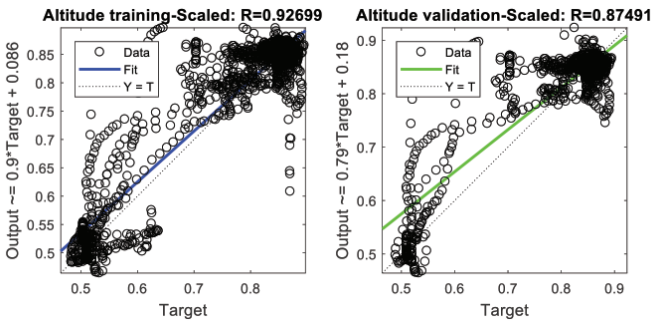
SNN: Shallow neural network

Figure 8. *Correlation coefficients, R, of NNM for training and validation altitude data*

Figure 9. *Comparison between SNN output and experimental pitch data for training and validation*

SNN: Shallow neural network

Figure 10. *Correlation coefficients, R, of the SNN model for training and validation pitch angle data*

SNN: Shallow neural network

Figure 11. *SNN model training data for heading motion*

SNN: Shallow neural network

Figures 5 and 6 show the depth-pitch motion modeling training and validation/test data, respectively. If the horizontal control surface, tailH, is sent saturated limit signals, it causes large amplitudes, as seen in Figure 5, with approximately 500 sampled data.

The correlation coefficient (R-value) is used to assess the outcomes of SNN model applications created with the aid of Matlab software. T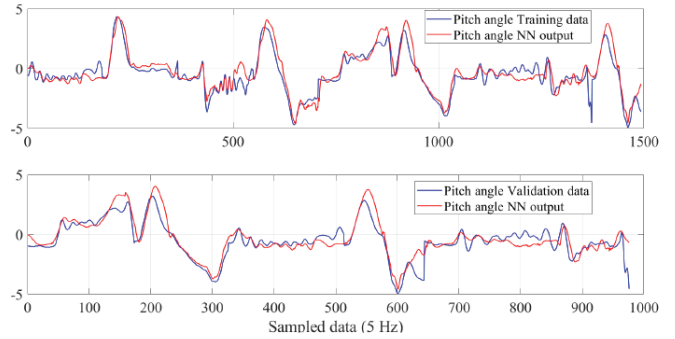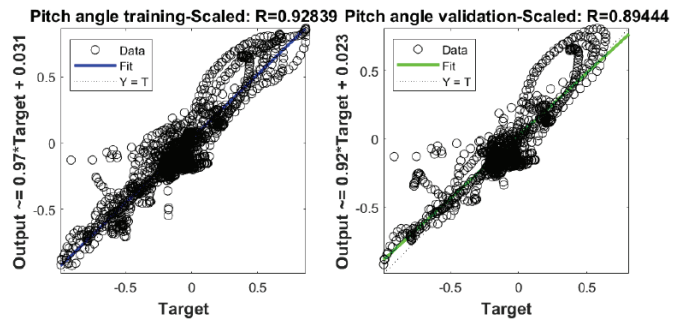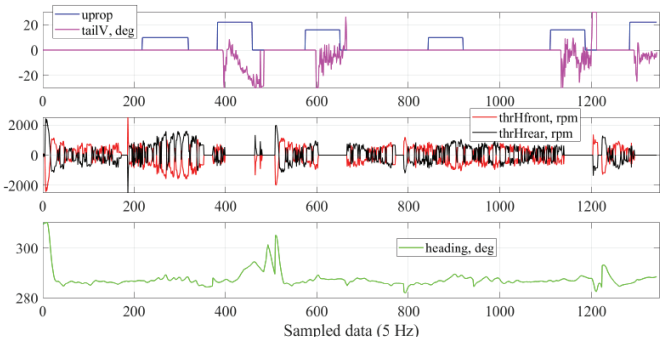he linear link between two continuous variables is measured by the R-value, which also indicates the direction of the association. The values fall between -1 and +1. This coefficient range can be interpreted as negligible if it falls between 0 and 0.09, weak if it falls between 0.1 and 0.39, moderate if it falls between 0.4 and 0.69, strong if it falls between 0.7 and 0.89, and very strong if it falls between 0.9 and 1.00 [30,31]. In the application results, the R-value is expressed as a proportional percentage.
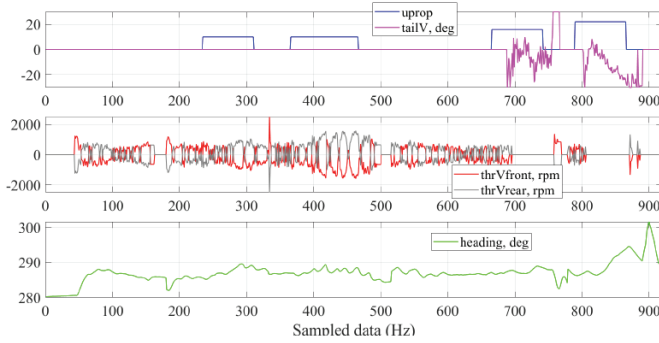
Figure 12. SNN model validation data for heading motion

SNN: Shallow neural network

Altitude and pitch motions of SNN depth-pitch model outputs have high R-values, approximately 90%. These comparisons between the SNN output and experimental test data and the R-values are shown in Figures 7-10.

Training and validation data for SNN heading motion modeling are given in Figures 10-12. A comparison between the SNN output and experimental heading data for training and validation is given in Figure 13. R-values, of SNN heading modeling training and validation outputs are 78% and 87%, respectively.

4. Dynamic Position Control

The PID controller is the most common type of closed-loop control system. These controllers continually monitor and modify a system's output to maintain a specified set point. The comparator loops back to the system output, y(t), and compares it to the set point, r(t), to produce the error signal, e(t)=r(t)-y(t). The closed-loop control reduces this error signal as much as possible before using it to produce the control signal u(t). The most general mathematical representation of the entire control function, Equations 1-4, can be represented as the sum of the three individual contributions [26].

$$u(t) = u_P(t) + u_I(t) + u_D(t) \tag{1}$$

$$u_P(t) = K_P * e(t) \tag{2}$$

$$u_I(t) = K_I * \int_0^t e(\tau)d\tau \tag{3}$$

$$u_D(t) = K_D * \frac{de(t)}{dt} \tag{4}$$

It is possible to find many methods in the literature regarding the adjustment of K_P, K_I, and K_D coefficients. The main adjustment method is the Ziegler-Nichols rule [32]. In practically adjusting these control coefficients,

the proportional K_P coefficient should first be adjusted according to the gain rate of the system. The K_P coefficient should be increased until the response of the system reaches the reference signal. In the second step, if there is a steady-state error in the system response, the integrative K_I coefficient should be increased/decreased until this steady-state error is eliminated. However, the disadvantage of increasing the integration coefficient is that delays and oscillations in the system response increase. In the third step, the derivative K_D coefficient may need to be adjusted to optimally adjust the system response time and oscillation.

There are two operating conditions in which depth-pitch control is used. The first involves modifying the type equation using a hover-style control method (at zero speed). Using vertical thrusters, the AUV depth and pitch may be changed. The second is a flight-style control approach that uses vertical thrusters for depth control and horizontal control surfaces (tails) for pitch motion reduction control. When operating across a wide range of speeds, the horizontal aft surfaces, ω_s, and the vertical tunnel thrusters, ω_{th}, offer a transition between the two control techniques. The integration (I) coefficient was the most effective in depth control based on simulation studies. When dealing with a significant shift in depth demand, an integrator for the generalized thrust control law may grow unreasonably large while the AUV is diving. The impact of the integral windup phenomenon is minimized using a conditional integration technique. The pitch for depth for hover-style and flight-style operations, proportional (P), integral (I)-derivative (D), and PI-D controls are used. It implemented a PI-D strategy instead of a PID to avoid a spike in the derivative term when changing the demand [2,6]. The Enhanced Differentiator (ED) approach was used to differentiate between variables and error variables [33]. If the ED algorithm is used for derivation, PID control can be used.
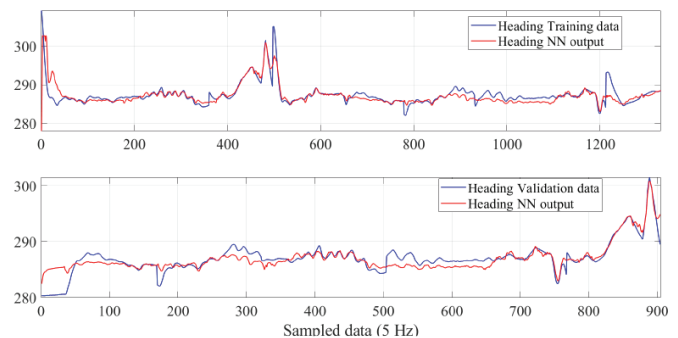

Figure 13. Comparison between SNN output and experimental heading data for training and validation

SNN: Shallow neural network

Due to their effectiveness and energy efficiency, the rudders (the vertical control surfaces for the Delphin2 AUV) are frequently used for heading control during high-speed operation. However, when operating in a low-speed regime where the control surfaces lose their effectiveness or when coping with significant heading mistakes, additional pressures from the horizontal tunnel thrusters are necessary. The AUV model can be maintained at the desired equilibrium with the help of the proportional (P)-derivative (D) (PD) function. Two cascade modules make up the heading control; the first module establishes a generalized moment for following heading demand, and the second module divides the generalized moment between the thrusters and rudders [34]. The horizontal thrusters and vertical control surfaces of the Delphin2 AUV model are responsible for distributing the generalized yaw moment [6]. The control signal can be applied in two ways for depth control, as Equations 5 and 6. The definitions of symbols are as follows; u_{c_total}, total control signal, u_{c_prev}, total control signal calculated one step earlier, Δu, calculated according to PD control. Conversely, u_c control signal can be calculated according to PID control.

$$u_{c\_total} = u_{c\_prev} + \Delta u \qquad (5)$$

$$u_c = u_{PID} \qquad (6)$$

The controller includes a two-layer PID controller so that the AUV vehicle can descend to the given reference depth while diving at zero speed, i.e., in a hover-style state. In the first layer, the total PD control signal, which calculates the total force required for the vehicle to dive to the reference depth, is calculated depending on the depth error. In the second layer, the dynamic change in the vehicle's longitudinal rotation center relative to the initial rotation center due to pitch error is calculated with PID control. Force allocation of the vertical thrusters is achieved with the PID control calculated in the second layer [6].

The control signal, according to Equation 5 and 6, was applied separately in the depth control of the AUV, while the altitude referenced 0.5 m, hover-style operation. A comparison of the two simulation results is shown in Figure 14. The result showed that the total PD control signal should be applied for depth control because when the vehicle reference altitude comes, the signal to the thrusters is not reset. The PID control signal method was applied in pitch motion control, as shown in Figure 15.

It is not possible to use the hover-style control approach at fast forward speeds. This is because as forward speed increases, thruster performance diminishes. As the AUV's speed increases, the thruster weight, w_{th}, decreases from

1 to 0. In this case, the total force calculated in the first layer required for the vehicle to dove in the hover-style condition multiplied by the thruster weight coefficient can be met by vertical thrusters in the flight-style condition. In addition, as the AUV's speed increases, the control surface, w_s, increases from 0 to 1. To calculate the horizontal control surface deflection for compensating pitch motion, the PID control equations are calculated in two layers. In the first layer calculation, the pitch bias, i.e., the reference value, is obtained by PID calculation, depending on the depth error of the vehicle. In the second layer, the deflection of the horizontal control surfaces is calculated using the PID calculation depending on the pitch error and multiplied by w_s according to the speed of the vehicle. The heading control problem includes two cascade modules. In the first module, the PID controller determines the total moment depending on the heading error. In the second module, the controller allocates the total moment between the horizontal thrusters and the vertical control surfaces based on the AUV speed. In addition, the moment sharing between front and rear horizontal thrusters should be calculated based on the changing center of rotation of the vehicle [6].

In addition, the control was applied for altitude referenced 0.5 m, flight-style operation. The control signal, according to Equation 5 and 6, was applied separately in the depth
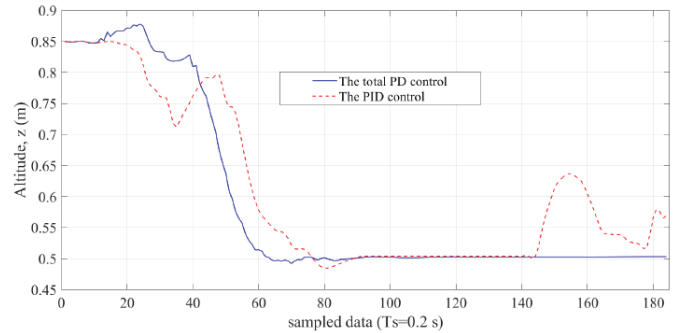

Figure 14. Altitude outputs of the control result data during altitude referenced 0.5 m, hover-style operation
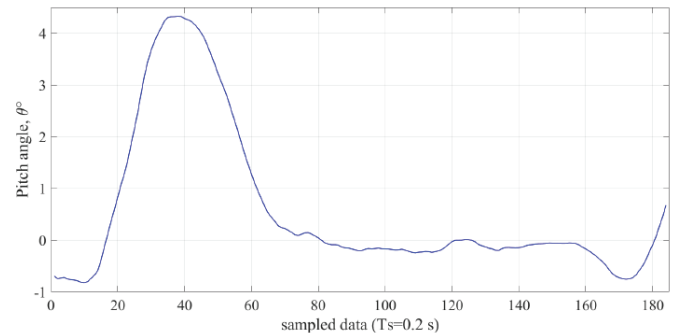

Figure 15. Pitch angle outputs of PID control result data during altitude referenced 0.5 m, hover-style operation

PID: Proportional integral derivative

control of the AUV, while the altitude referenced 0.5 m, flight-style operation. A comparison of the two simulation results is shown in Figure 16. The outcome demonstrated that the total PD control signal should be used for depth control because the signal to the thrusters is not reset when the vehicle reference altitude arrives, as shown in Figure 17. The PID control signal method was applied to pitch and heading motion control. The other simulation results are shown in Figures 18-20.

5. Conclusions and Proposed Methods

5.1. Conclusions

An over-actuated design enabled the AUV model to perform various missions, spanning from hover-style operation at zero or slow speeds to flight-style operation at forward speeds up to approximately 1 m/s. The current heading and turning rates were obtained from the IMU at a sample rate of 20 Hz. Surge and sway motions used in the control systems were estimated as dead reckoning using the dynamics model at 20 Hz to comply with the IMU, whereas the control systems were implemented at 5 Hz so that they could synchronize to the sensor and actuator interfacing nodes. However, the localization calculation based only on the dynamic model, without DVL measuring the speed of the AUV, caused drifts, and this case negatively affects the running control algorithms.
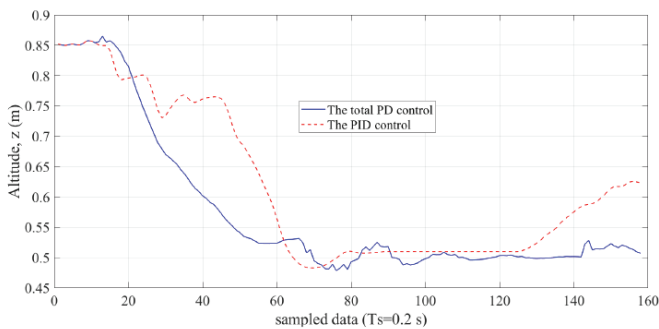

Figure 16. Altitude outputs of the control result data during altitude referenced 0.5 m, flight-style operation
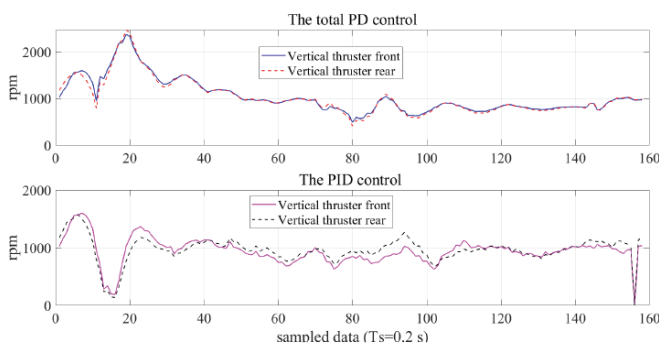

Figure 17. Vertical thruster front outputs of the control result data during altitude referenced 0.5 m, flight-style operation

The depth of the AUV was measured using both an echo-sounding altimeter and a pressure sensor. The depth pressure sensor was negatively affected by the vertical tunnel thrusters, and its signal was very unstable and noisy. The altimeter output signal was more stable than the pressure depth sensor output; therefore, the altimeter output signal data were used for depth-pitch control.

The depth-pitch and PD heading motion operations were performed for each mission operation in the tank tests. Feedback signals were collected in the tank tests from
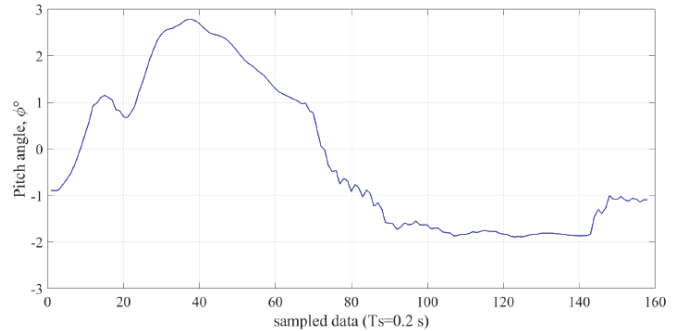

Figure 18. Pitch angle outputs of PID control result data during altitude referenced 0.5 m, flight-style operation
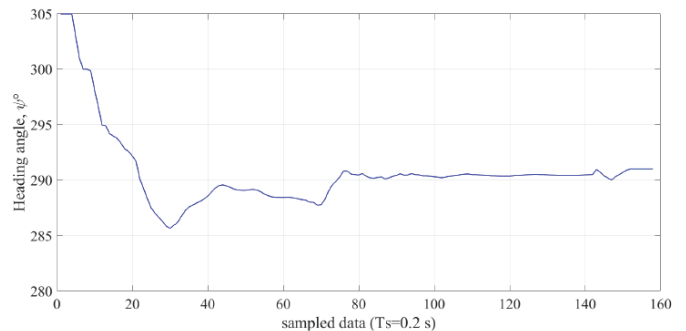
PID: Proportional integral derivative

Figure 19. Heading angle outputs of PID control result data during altitude referenced 0.5 m, flight-style operation
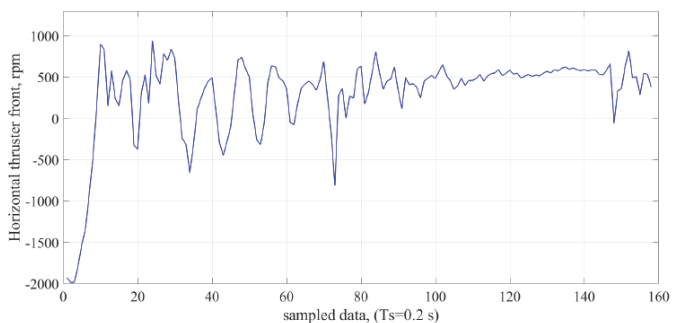
PID: Proportional integral derivative

Figure 20. Horizontal thruster front outputs of PID control result data during altitude referenced 0.5 m, flight-style operation

PID: Proportional integral derivative

the sensors, altimeter, pressure depth sensor, and IMU, according to set values on the actuator, including the vertical and horizontal tunnel thrusters, the vertical and horizontal control surfaces as the tails, and the propeller. The input-output test data were used to form nonlinear coupled mathematical models. The models were formed in two groups as depth-pitch motion and heading motion black-box models using the SNN algorithm. The SNN R-value, of the depth-pitch motion SNN model and the SNN R-value, of the heading motion SNN model were approximately 0.90 and 0.80, respectively. This nonlinear coupled mathematical model was used to develop the control design.

The control process was applied for altitude-referenced 0.5 m, hover-style, and flight-style operations. The control signal, according to the total PD and PID control, was applied separately in the depth control of the AUV. The outcome demonstrated that the total PD control signal should be used for depth control because the signal to the thrusters is not reset when the vehicle reference altitude arrives. The PID control signal method was applied to pitch and heading motion control. Good performance was obtained in the simulation studies. To achieve better results in every mission, there is a need to study an advanced control algorithm in the future.

5.2. Proposed Methods

The Delphin2 software's dead reckoning technique results in AUV motion drifts. The DVL/IMU measuring system can be employed because of less drift. Because of wall effects, USBL and LBL measurement equipment do not function properly in tanks. In addition, the AUV's localization range (about 30 cm) when using vision feedback from a laser and camera is relatively small.

To locate the AUV during tank testing, it has been recommended to integrate two or three echo-sounding altimeters with the IMU and a pressure depth sensor on the AUV. An AUV can measure the x- and y- axes positions when two echo-sounding altimeters are added. The frequency range of the altimeter is 1-4 Hz. If a magnetometer displays large drifts during tank tests, three-echo-sounding altimeters can also identify the yaw angle. Furthermore, DVL is more expensive than an altimeter that emits an echo [35].

In addition, an echo-sounding altimeter would be used to maintain distance control on AUVs in real-world circumstances, such as during the flight of AUVs in shallow coastal and under-ice areas, as well as during AUV docking, because the USBL measurement system might not work properly close to shore. Both stationary and moving targets might aid in avoiding AUV collisions.

References

[1] J. Liu, et al. *Design and Control of a Flight-Style AUV with Hovering Capability*: In Proceedings of the International Symposium on Unmanned Unethered Submersible Technology (UUST 2009), pages 1-9, Durham NH, USA. Autonomous Undersea Systems Institute (AUSI), 2009.

[2] A. B. Phillips, et al. "Delphin2: an over actuated autonomous underwater vehicle for manoeuvring research." *Transactions of The Royal Institution of Naval Architects Part A. International Journal of Maritime Engineering*, vol. 155, pp. 171-180, 2013.

[3] L. V. Steenson, *Experimentally Verified Model Predictive Control of a Hover-Capable AUV*. PhD thesis, University of Southampton, UK, 2013.

[4] L. V. Steenson, et al. "Model predictive control of a hybrid autonomous underwater vehicle with experimental verification," *Proceedings of the Institution of Mechanical Engineers, Part M: Journal of Engineering for the Maritime Environment*, vol. 228, pp. 166-179, Feb 2014.

[5] S. M. Schillai, S. R. Turnock, E. Rogers, and A. B. Phillips, "Evaluation of terrain collision risks for flight style autonomous underwater vehicles," *Published in: 2016 IEEE/ OES Autonomous Underwater Vehicles (AUV),* Tokyo, Japan, 2016, pp. 311-318.

[6] K. Tanakitkorn, *Guidance, Control and Path Planning for Autonomous Underwater vehicles*. Ph.D. thesis, University of Southampton, UK, 2017.

[7] M. Ertogan, P. A. Wilson, G. T. Tayyar, and S. Ertugrul, "Optimal trim control of a high-speed craft by trim tabs/interceptors Part I: Pitch and surge coupled dynamic modelling using sea trial data," *Ocean Engineering*, vol. 130, pp. 300-309, Jan 2017.

[8] C. G. Karras, D. J. Panagou, and K. J. Kyriakopoulos, "Target-referenced localization of an underwater vehicle using a laser-based vision system," in *IEEE, OCEANS, Boston, MA, USA, 2006*.

[9] G. C. Karras, and K. J. Kyriakopoulos, "Localization of an underwater vehicle using an IMU and a laser-based vision system," in *IEEE, Mediterranean Conference on Control and Automation, Athens-Greece, 2007*.

[10] G. C. Karras, S. G. Loizou, and K. J. Kyriakopoulos, "Towards semi-autonomous operation of under-actuated underwater vehicles: sensor fusion, on-line identification and visual servo control." *Autonomous Robots*, vol. 31, pp. 67-86, May 2011.

[11] C. Cain, and A. Leonessa, "Laser based rangefinder for underwater applications." in *Proceedings of the American Control Conference American Control Conference, (ACC), 2012 Canada*, pp. 6190-6191, 2012.

[12] D. R. Romagos, *Underwater SLAM for structured environments using an imaging sonar*. Ph.D. thesis, Department of computer Engineering, University of Girona, Spain, 2008.

[13] A. Burguera, Y. Gonzalez, and G. Oliver, "The UspIC: performing scan matching localization using an imaging sonar," *Sensors*, vol. 12, pp. 7855-7885, Jun 2012.

[14] A. J. Plueddemann, A. L. Kukulya, R. Stokey, and L. Freitag, "Autonomous underwater vehicle operations beneath coastal sea ice," *IEEE/ASME Transactions on Mechatronics*, vol. 17, pp. 54-64, Feb 2012.

[15] D. Bandara, Z. Leong, H. Nguyen, S. Jayasinghe, and A. L. Forrest, "Technologies for underwater-ice AUV navigation." *2016 IEEE/ OES, Autonomous Underwater Vehicles (AUV),* Tokyo, Japan, 2016.

[16] L. Chen, S. Wang, K. McDonald-Maier, and H. Huosheng, "Towards autonomous localization and mapping ofAUVs: a survey," *International Journal of Intelligent Unmanned Systems*, vol. 1, pp. 97-120, May 2013.

[17] L. Paull, S. Saeedi, M. Seto, and L. Howard Li, "AUV navigation and localization: a review," *IEEE Journal of Oceanic Engineering*, vol. 39, pp. 131-149, Jan 2014.

[18] C.-M. Lee, P.-M. Lee, S.-W. Hong, and S.-M. Kim, "Underwater navigation system based on inertial sensor and doppler velocity log using indirect feedback Kalman Filter," *International Journal of Offshore and Polar Engineering*, vol. 15, pp. 8895, Jun 2005.

[19] J. Davis, I. Tena, "Dynamic positioning of underwater vehicles (tethered or not)," *Dynamic Positioning Conference, Dynamic Positioning Committee, Marine Technology Society*, pp. 1-15, 2008.

[20] S. Liu, D. Wang, E. K. Poh, and Y. Wang, "Dynamic positioning of AUVs in shallow water environment: obeserver and controller design," in *Proceedings of the IEEE/ASME, International Conference on Advanced Intelligent Mechatronics, Monterey, California,* pp. 705-710, 2005.

[21] A. P. Aguiar, and A. M. Pascoal, "Dynamic positioning and way-point tracking of underactuated AUVs in the precence of ocean currents," in *Proceedings of the 41st IEEE, Conference on Decision and Control Las Vegas, Nevada USA*, pp. 2105-2110, 2002.

[22] S. Zhao, *Advanced control of autonomous underwater vehicles*, PhD thesis, The University of Hawai, USA, 2004.

[23] N. Miskovic, Z. Vukic, I. Petrovic, and M. Barisic, *Distance keeping for underwater vehicles – tuning Kalman Filters using self-oscillations,* IEEE, OCEANS 2009-EUROPE, 11-14 May 2009.

[24] J. Gao, C. Liu, and A. Proctor, "Nonlinear model predictive dynamic positioning control of an underwater vehicle with an onboard USBL system." *Journal of Marine Science and Technology,* vol. 21, pp. 57-69, Aug 2015.

[25] S. D. McPhail, "Autosub6000: A Deep Diving Long Range AUV," *Journal of Bionic Engineering*, vol. 6, pp. 55-62, Mar 2009.

[26] L. Ljung, *System identification: theory for the user*, Prentice Hall, Second Edition, 1999.

[27] D. E. Rumelhart, C. E. Hinton, and R. J. Williams, "Learning Internal Representations by Error Propagation," in *Parallel Distributed Processing: Explorations in the Microstructures of Cognition*, vol. 1, Cambridge, MA: MIT Press, 1986.

[28] C. C., Yu, and B. D. Liu, "A backpropagation algorithm with adaptive learning rate and momentum coefficient." in *Proceedings of the 2002 International Joint Conference on Neural Networks. IJCNN'02 (Cat. No. 02CH37290), IEEE, 2002.* vol. 2, pp. 1218-1223, 2002.

[29] H. Demuth, and M. Beale, *Neural Network Toolbox for use with Matlab*. User's Guide Version 4, 2004.

[30] M. G. Kendall, *The Advanced Theory of Statistics,* 4th Ed., Macmillan, 1979.

[31] J. Frost, *Introduction to statistics: an intuitive guide for analyzing data and unlocking discoveries*, Statistics by Jim Publishing, 2020.

[32] K. Ogata, *Modern Control Engineering*, Fifth Edition. Pearson Education, Inc., publishing as Prentice Hall, New Jersey, 2010.

[33] Y. X. Su, C. H. Zheng, P. C. Mueller, and B. Y. Duan, "A simple improved velocity estimation for low-speed regions based on position measurement only," *IEEEE Transactions on Control Systems Technology*, vol. 14, pp. 937-942, Sep 2006.

[34] T. I. Fossen, T. Johansen, "A survey of control allocation methods for ships and underwater vehicles," in *2006 14th Mediterranean Conference on Control and Automation*, IEEE, 2006, pp. 1-6.

[35] M. Ertogan, G. T. Tayyar, P. A. Wilson, and S. Ertugrul, "Marine measurement and real-time control systems with case studies," *Ocean Engineering*, vol. 159, pp. 457-469, 2018.